Design of membrane actuators based on ferromagnetic shape memory alloy composite for the synthetic jet actuator

Yuanchang Liang[a], M. Taya[a], Yasuo Kuga[b]
[a]Center for Intelligent Materials and Systems, Department of Mechanical Engineering, University of Washington, Seattle, WA 98195-2600, USA;
[b]Department of Electrical Engineering, University of Washington, Seattle, WA 98195-2500, USA

ABSTRACT

A new membrane actuator based on our previous diaphragm actuator was designed and constructed to improve the dynamic performance. The finite element analysis was used to estimate the frequency response of the composite membrane which will be driven close to its resonance to obtain a large stroke. The membrane is made of ferromagnetic shape memory alloy (FSMA) composite including a ferromagnetic soft iron pad and a superelastic grade of NiTi shape memory alloy (SMA). The actuation mechanism for the FSMA composite membrane of the actuator is the hybrid mechanism that we proposed previously. This membrane actuator is designed for a new synthetic jet actuator package that will be used for active flow control technology on airplane wings. Based on the FEM results, the new membrane actuator system was assembled and its static and dynamic performance was experimentally evaluated including the dynamic magnetic response of the hybrid magnet.

Keywords: shape memory alloy, active flow control, ferromagnetic, synthetic jet, superelasticity, martensitic transformation, hybrid mechanism, composite, hybrid magnet

1. INTRODUCTION

The synthetic jet actuator is to help aircraft improve aerodynamic performance and stabilize flights at low Mach number by injecting high momentum air into the airflow on aircraft wings [1-8]. The active flow control can be achieved by injecting synthetic jets with high momentum air into the flow at the appropriate locations on aircraft wings. For example, the Boeing company has applied active flow control technology to rotorcraft, V22, focusing on alleviating rotor download on tiltrotor aircraft, for increasing the V22 mission capability on both payload and range [7,8]. Currently, most of the synthetic jet actuators have been constructed based on piezoelectric materials as actuator materials to produce synthetic jet flow [5-8]. However, piezoelectric materials may not produce large force to induce strong jet flow. Therefore, we are seeking another design approach of a synthetic jet actuator with a vibrating surface based on ferromagnetic shape memory alloy composite and the hybrid mechanism.

Ferromagnetic shape memory alloys (FSMA) have been studied for possible applications of fast responsive and high power, yet light weight actuators controlled by magnetic field [9-11]. However, it is disadvantageous to use uniform (constant) magnetic field alone to drive FSMAs because it has been found to produce small force [12-14]. Therefore, we proposed the hybrid mechanism that is adopted [14-16] in the present study of membrane actuators for the application to the synthetic jet actuator. The hybrid mechanism is based on the stress-induced martensitic phase transformation produced by applied magnetic field gradient, thus enhancing the displacement, as the stiffness of shape memory alloy reduces due to the martensitic phase transformation. We have designed the diaphragm actuator based on the composite material made of superelastic grade of NiTi shape memory alloy and ferromagnetic soft iron as a composite diaphragm driven by a hybrid magnet system [17,18]. The diaphragm actuator has been fabricated based on the hybrid mechanism [18]. It was designed by both mechanical and ferromagnetic finite element analyses, followed by the assembly of the actuator with one-side FSMA composite diaphragm (0.4 in thickness and 100mm in diameter). The quasi-static performance of the diaphragm actuator was measured experimentally about 3mm stroke with 3 Amp input current. However the performance under dynamic loading was only 6Hz with 1.5mm peak to peak stroke on the composite diaphragm. This test was done under the AC signal which will waste half of the input power because due to the character of the hybrid magnet system. To increase the frequency response and conserve energy for the applications of

Smart Structures and Materials 2004: Smart Structures and Integrated Systems, edited by Alison B. Flatau, Proc. of SPIE Vol. 5390 (SPIE, Bellingham, WA, 2004)
0277-786X/04/$15 · doi: 10.1117/12.540100

synthetic jet, it is necessary to optimize the membrane actuator design for dynamic loading including the mechanical performance of the composite diaphragm and the driving units. This paper will present the proposed synthetic jet actuator package, dynamic finite element analysis of the new FSMA composite diaphragm as well as experimental results of static and dynamic testing of the membrane actuator. The goal of the membrane actuator is to produce reasonable stroke with higher frequency, hence, can be applied to active flow control technology.

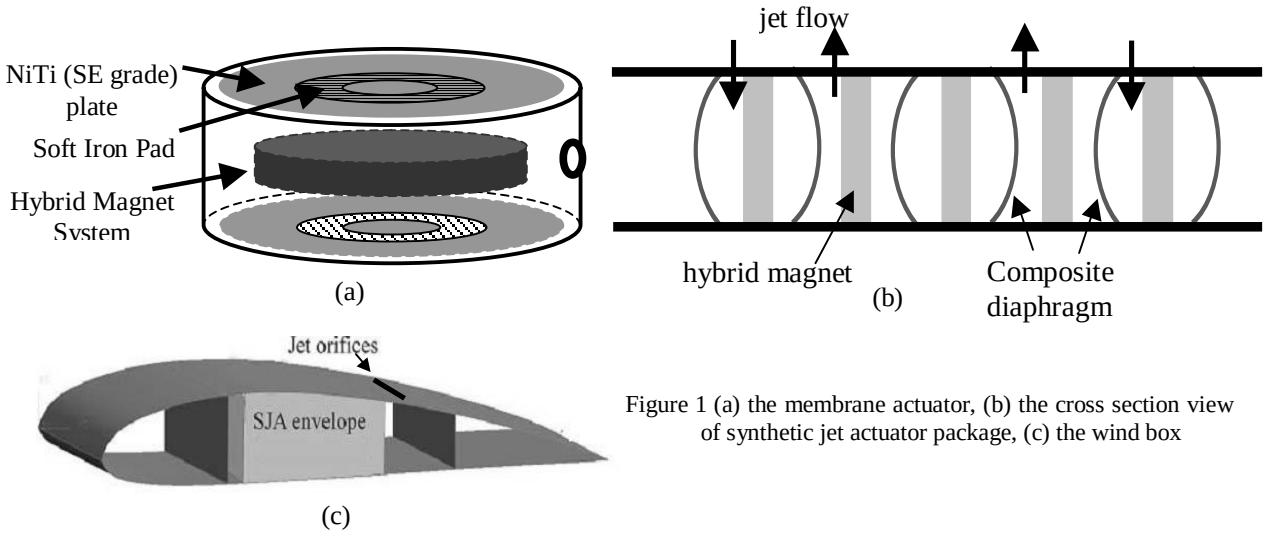

Figure 1 (a) the membrane actuator, (b) the cross section view of synthetic jet actuator package, (c) the wind box

2. SYNTHETIC JET ACTUATOR PACKAGE

The membrane actuators mainly consist of hybrid magnet systems and FSMA composite diaphragms [18] as shown in Fig. 1(a). The hybrid magnet includes yoke, magnet coil and permanent magnet, which can drive two composite diaphragm on both sides. It has been shown that the hybrid magnet system is more efficient and produces much larger force than a traditional solenoid magnet [17,18]. The FSMA composite diaphragm is composed of a superelastic grade NiTi SMA thin plate and a ferromagnetic soft iron pad. Therefore, the synthetic jet actuator package can be built including several membrane actuators with multiple chambers as shown in Fig. 1(b). This FSMA composite diaphragm will be driven by the hybrid magnet system based on the hybrid mechanism; the stress-induced martensitic phase transformation produced by applied magnetic field gradient, thus enhancing the displacement, as the stiffness of shape memory alloy reduces due to the martensitic phase transformation. The hybrid magnet will create a very high gradient of magnetic field and induce a large force on the soft iron pad. Therefore, the diaphragm will vibrate and create a jet flow, as shown in Fig. 1(b). To increase the stroke of the composite diaphragm, it will be designed to oscillate close to its resonance frequency. The closer to the resonance frequency, the larger stroke of the vibration which can create larger volume change in each membrane chamber and induce higher momentum of the jet flow. However, the larger stroke will also induce larger stress on the diaphragm. The merit of using superelastic NiTi plate as the diaphragm is because it can sustain high stress level without permanent deformation as well as we can obtain larger stroke when the stress level on the diaphragm is over the pseudo-yield stress of the superelasticity. In the future, the synthetic jet actuator package will be mounted into the envelope of the wind box (Fig. 1(c)) for the wind tunnel testing. The jet flow will be controlled by the orifices on the wing surface to increase the cruse lift and the angle of attack.

3. DYNAMIC ANALYSIS of COMPOSITE DIAPHRAGM

The estimation of the dynamic analysis of the composite diaphragm is based on the finite element analysis. Figure 2 (a) and (b) shows the dimensions of the composite diaphragm used for the membrane actuator and the quarter diaphragm as the FEM model, respectively. Because of the limitation of the FEM program which can not perform the frequency response calculation with non-linear stress-strain relationship of superelasitcity, this estimation is only valid before the stress-induced martensitic transformation (at 380 MPa) on the NiTi plate. The Young's modulus of 70GPa, poisson ratio of 0.33 and density of 6500 Kg/m^3 are used as the input data for the NiTi plate. The Young's modulus of 210GPa,

poisson ratio of 0.33 and density of 7850 Kg/m^3 are used for the soft iron pad. The boundary condition at the gripping potion is assumed without slipping and rotation. Figure 3 (a) shows the resonance frequency as a function of NiTi plate thickness where the composite diaphragm has the same dimensions as Fig. 2(a) except the plate thickness. It clearly shows that the thicker the plate, the higher the resonance frequency becomes. The thickness of the soft iron pad also can change the resonance frequency of the composite diaphragm. Figure 3(b) shows that use of the thicker soft iron pad, results in lowering the resonance frequency of the composite diaphragm. Since the designated frequency of driving the diaphragm is around 100 Hz, the plate thickness of 0.3mm and the pad thickness of 5mm are used. This means that we would like to drive the composite diaphragm close to the resonance frequency of 151Hz to obtain a larger stroke on the diaphragm.

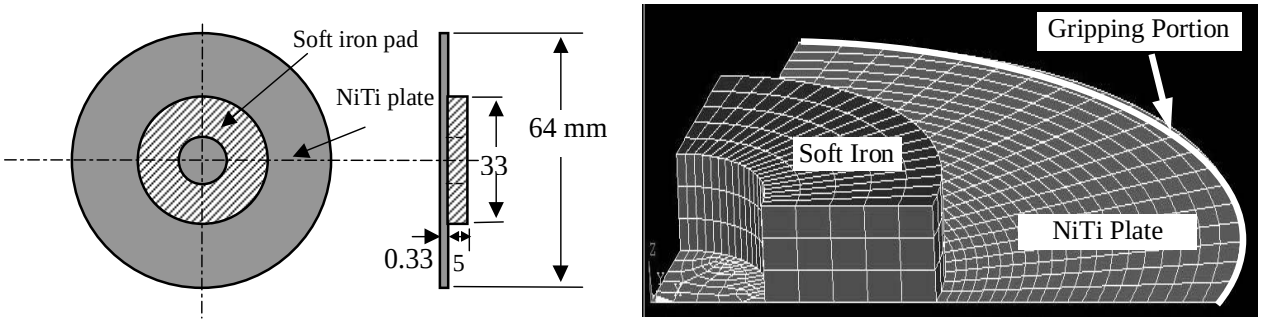

Figure 2 (a) the dimensions of the composite diaphragm, (b) the quarter composite diaphragm as the FEM model.

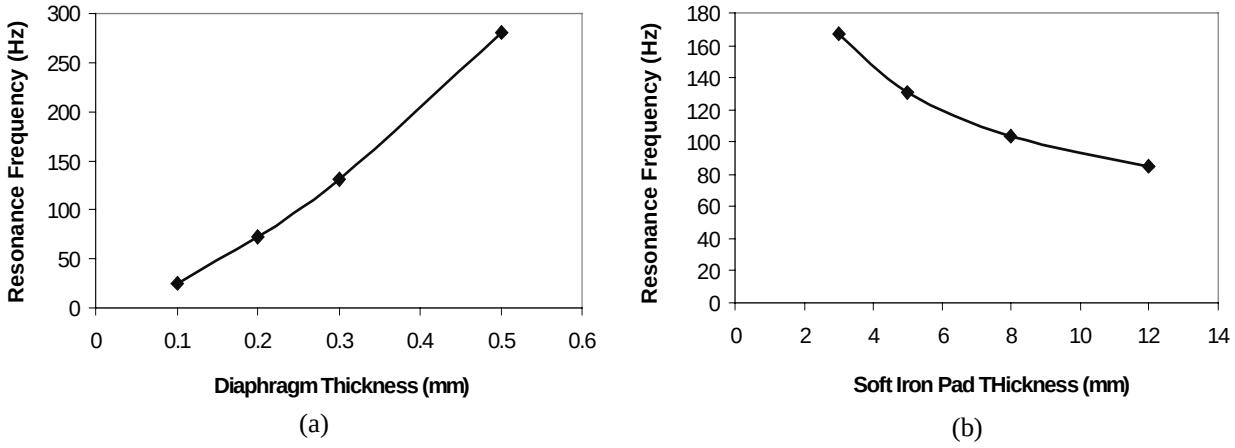

Figure 3 (a) the NiTi plate thickness and (b) the soft iron pad thickness estimated by FEM as a function of resonance frequency

The estimated frequency response of the FSMA composite diaphragm with the configuration in Fig.2(a) has been done by FEM. The results of the stroke on the center of the diaphragm as a function of frequency are shown in Fig. 4(a). The stroke will significantly increase as the frequency close to 150 Hz where the resonance frequency of the diaphragm is around 151Hz. As we mentioned previously, the finite element analysis is limited by its input data. It can not carry the analysis with a non-linear stress-strain curve of the material such as the superelastic NiTi SMA. Therefore, this analysis result only gives us a designing guidance of the composite diaphragm frequency we can drive. However, the analysis results are still valid before the stress-induced martensitic transformation. Figure 4(b) shows the stress level on several locations of the diaphragm as a function of frequency. The highest stress level occurs on both locations of gripping potion and the interface between the NiTi plate and the soft iron pad as shown in Fig.2 (b). The arrow indicates the onset of the stress induced martensitic transformation where the calculation is still valid. It is about 380 MPa when the frequency is 145 Hz and the stroke of the diaphragm is about 4mm (about 8mm peak to peak stroke). This also means

that when the stress-induced martensitic transformation occurs, more stroke we can obtain from the composite diaphragm because the stiffness of the NiTi plate decreases due to the transformation. Further, the synthetic jet flow velocity can be estimated by the mass rate conservation:

$$v = \frac{\nabla V \times f}{W \times L} \tag{1}$$

where v is the jet velocity, f is the vibrating frequency of the diaphragm and W is the width and L is the length of flow entrance/exit slot. The deformation of the diaphragm is like a corn shape as shown in Fig. 7 where r1 and r2 are the radius of NiTi plate and soft iron pad, respectively and h is the stroke of the diaphragm. For the current membrane actuator design (r1 = 32 mm, r2 = 16.5 mm, h = 4 mm, f = 145 Hz), if the slot has W = 1 mm, L = 40 mm, the jet velocity is estimated about 30 m/s.

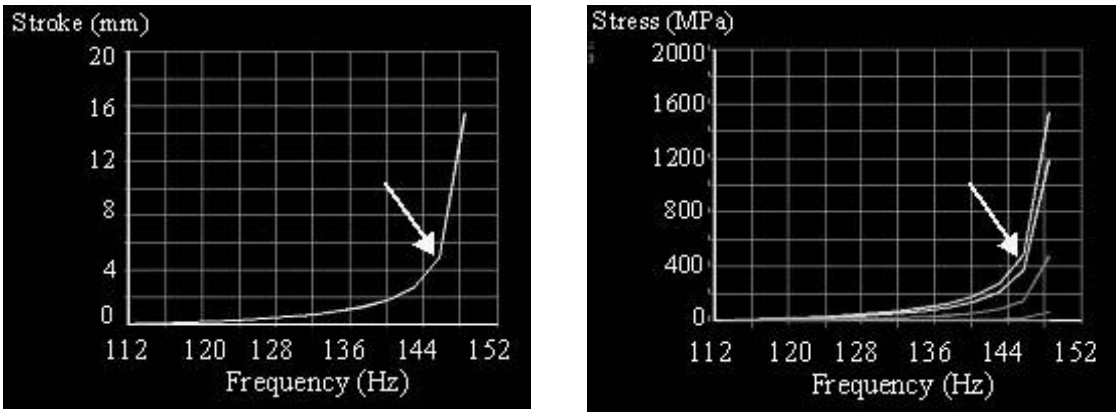

(a) (b)

Figure 4 Finite element results of frequency response of the composite diaphragm (a) stroke and (b) stress level as the function of frequency

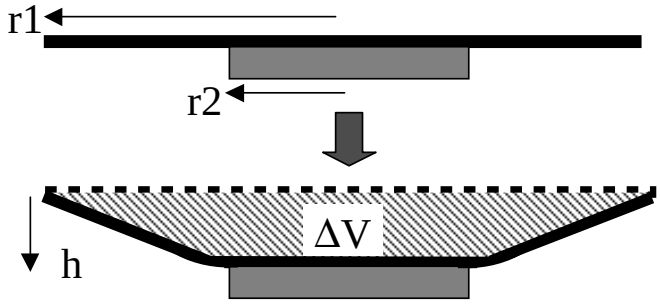

Figure 5 schematic of the deformation of the composite diaphragm

4. PERFORMANCE OF THE ACTUATOR SYSTEM

4.1 Testing system and components of the actuator

The testing system includes two function generators, a power supply, an amplifier and a laser displacement measurement system. The amplifier can provide two square wave signals for 2 hybrid magnet systems. The magnitude of the square wave signal is between 0 and 20V. This can save more energy because the hybrid magnet can only operate for one direction of the electrical current flow. Function generators control the frequency of signals and their signal phases are adjustable between these two function generators. The laser displacement measurement system can control the position of the laser device along the diameter of the diaphragm so the profile of the diaphragm is detected. This information can

help us to calculate how much volume changes during the deformation of the FSMA composite diaphragm. Both quasi-static and dynamic tests of the membrane actuator system will be performed.

The final assembly of the membrane actuator system is shown in Fig. 6(a). The composite diaphragm will be placed at the center between two hybrid magnets (Fig. 6(b)) where each hybrid magnet can drive 2 diaphragm for the future synthetic jet actuator package as shown in Fig. 1(b). The FSMA composite diaphragm has been made of a superelastic NiTi plate and a soft iron pad as shown in Figure 2(a). The NiTi plate is about 0.33mm in thickness and 64mm in diameter. The soft iron pad is about 33mm in outer diameter, 3mm in inner diameter and 6mm in thickness. The connection between the NiTi plate and the soft iron pad is established by several screws with reinforcement of an aluminum ring on the opposite side of the plate. A driving unit, the hybrid magnet system, was assembled and each is about 50mm in height and 72mm in diameter. Both pad and yoke are made of low carbon steel.

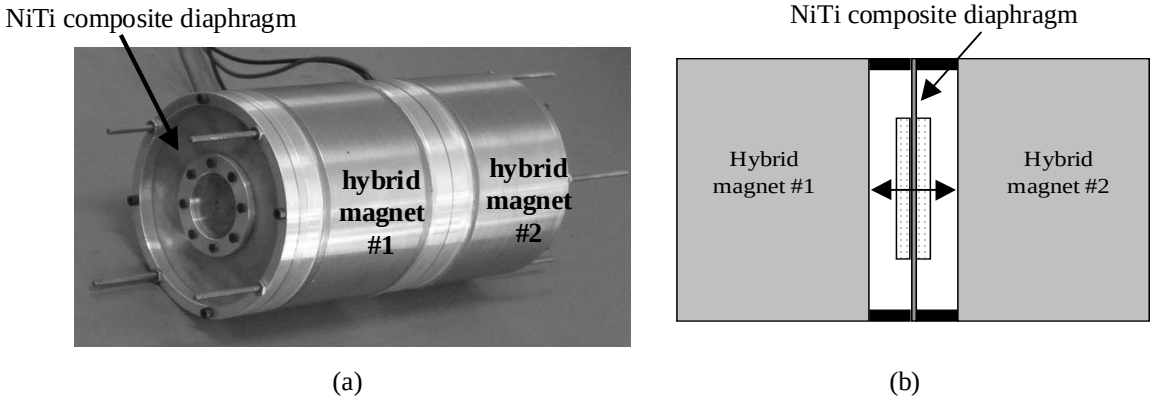

Figure 6 (a) the membrane actuator and (b) its cross section view

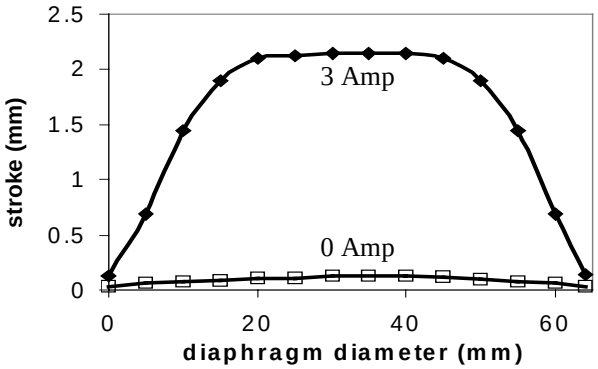

Figure 7 Profile of the deformed composite diaphragm under a quasi-static loading

4.2 Performance of the actuator

The quasi-static test of the membrane actuator is performed with one hybrid magnet and a maximum input current about 3 Amp for the system. The profile across the diameter of the FSMA composite diaphragm was then detected by the laser measurement system as shown in Fig. 7, where the black and gray filled symbols represent cases of with and without input current, respectively. This test result indicates that the hybrid magnet system with 3 Amp is powerful enough to deform the FSMA composite diaphragm. The composite diaphragm has a 2mm displacement when the hybrid magnet system is active. When the power is off, the FSMA composite diaphragm will spring back due to the superelastic property of the NiTi shape memory alloy plate. If a larger current input is available, larger force can be induced by the hybrid magnet system and more deformation of the composite diaphragm will occur.

The dynamic performance on the diaphragm actuator was tested as well. Due to the structure of the membrane actuator, the stroke of the composite diaphragm can not be detected by the laser measurement. Nevertheless, the stroke still can be detected by a CCD camera. Two square wave signals of 20V are generated from the function generators and the amplifier. When the signal frequency is 20Hz, 4mm peak to peak stroke of the composite diaphragm is detected. However, the composite diaphragm inclined to one side of the hybrid magnet and the stroke did not increase when we increase both the signal frequency and the voltage. This is due to a large amount of eddy currents induced in the yoke of the hybrid magnet system which will cause energy loss and reduce the actuator efficiency. The further examination of eddy currents will be discussed in the next section.

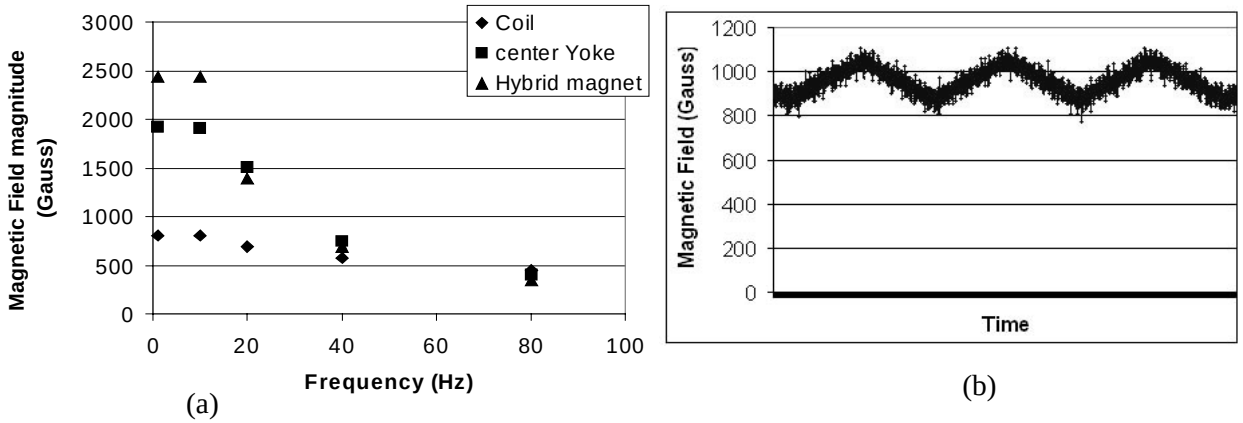

Figure 8 (a) frequency response of the magnetic field produced by coil, coil with center yoke and hybrid magnet (b) the magnetic field produced by the hybrid magnet is measured at 80 Hz

5. DISCUSSION

The dynamic performance of the membrane actuator improved from our previous diaphragm actuator [18]. A 4mm peak to peak stroke of the membrane actuator was obtained with input signal of 20V and 20 Hz. However, the stroke decreases when the frequency increases as well as the input voltage increases. This is due to the occurrence of eddy currents which is evidenced by the center yoke of the hybrid magnet getting hot after several dynamic testing. The produced magnetic field from a coil, a coil with a center yoke and the hybrid magnet were measured by a teslameter as a function of frequency. The results are shown in Fig. 8(a). The magnetic field magnitude on the vertical axis is the peak to peak value of the measured magnetic field. The results indicate that the magnetic field slightly drop in the coil when the frequency is over 20 Hz while the magnetic fields of center yoke and the hybrid magnet decline significantly. When the frequency is 80Hz, the magnetic fields are almost the same for three cases. This means the eddy-current effect is too large to let the magnetic flux flowing through the yoke. Figure 8(b) further shows the measurement on the hybrid magnet at 80Hz near the location of the permanent magnet. The magnetic field is not reset to zero when the signal is zero. This means the force will always generate on the composite diaphragm and the diaphragm will not spring back to the neutral position. This is why the diaphragm inclined to one of the hybrid magnets as described in section 4.2. Figure 8(a) also implies that the turns of the coil should be reduced to increase its efficiency because the magnetic field produced by the coil slightly decreases when the signal frequency is 80 Hz.

To increase the efficient of the hybrid magnet for higher frequency, the eddy currents can be reduced by using laminated yoke in a plane perpendicular to the direction of the eddy currents and small-distributed coils. A simple setup of a hybrid magnet has been made as shown in Fig. 9(a). The yoke and the armature are laminated. There are 5 coils, electrically connected in parallel but magnetically connected in series along the yoke. The hollow black circle is the point of measuring magnetic field. The input voltage (Peak to Peak) is about 34V. Fig. 9(b) shows the experimental results of the magnetic field magnitude as a function of frequency. It shows the system has a great improvement on the frequency response even up to 140 Hz. The magnitude of magnetic field at low frequency in Fig. 9(b) is smaller than the magnitude in Fig. 8(a) because the hybrid magnet as shown in Fig. 9(a) is not optimized yet. However at higher

frequency over 40 Hz, the hybrid magnet system with small-distributed coils and laminated yoke has better frequency response and has larger magnetic field. This means that the hybrid magnet can be improved for the usage of higher frequency and the stroke of the membrane actuator can be increased, therefore, induce higher momentum of synthetic jet flow.

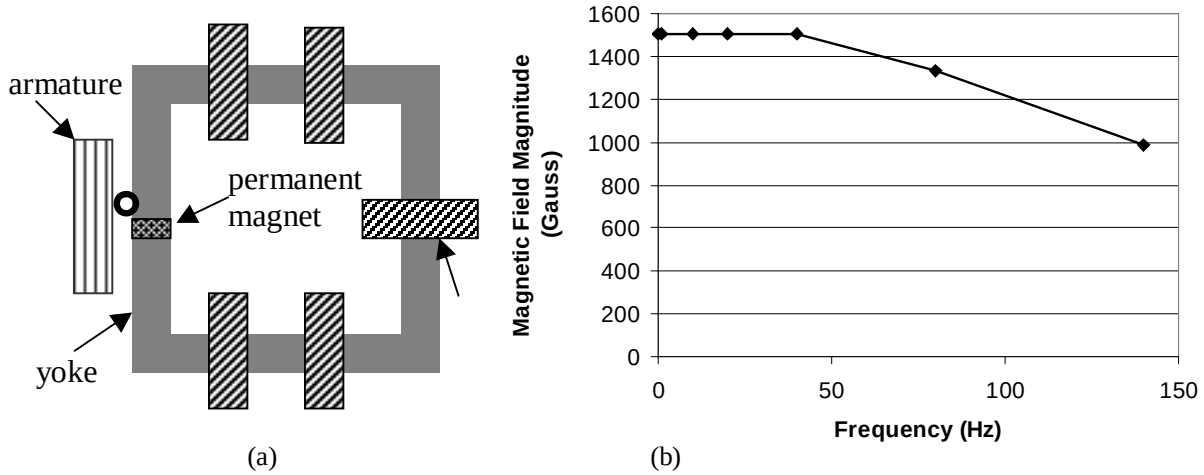

(a) (b)

Figure 9 (a) The setup of hybrid magnet with small-distributed coils and laminated yoke, (b) the magnetic field response at the hollow black circle in (a).

6. CONCLUSION

A new membrane actuator system was built based on the hybrid mechanism to improved the previous version of the diaphragm actuator made of ferromagnetic shape memory alloy (FSMA) composite, i.e. NiTi/soft iron. The quasi-static performance of the actuator was measured experimentally about 2mm stroke. Its dynamic performance improved with a 4 mm peak to peak stroke under 20 Hz loading. Because of eddy current effect, the efficiency of the hybrid magnet decreases and the stroke of the membrane actuator become small. However, we also showed that the hybrid magnet system can be further improved by laminating the yoke and using distributed small coils. We are currently working on the revised design of the driving unit based on laminated yoke for a new SJA package, with which the magnetic performance of the driving unit is expected to increase toward higher frequencies, hence, the stroke of the actuator increases for higher signal frequency and voltage. It is expected that a new synthetic jet actuator can be designed based on the membrane actuator composed of FSMA composite and hybrid magnet system.

ACKNOWLEDGEMENTS

This study was supported by DARPA-ONR contract (N-00014-00-1-0520). Dr. Roshdy Barsoum of ONR and Dr. John Main of DARPA are the program monitors. The present authors are thankful to Boeing Company (Mr. Ed White and Dr. Dale Pitt) for their advice on synthetic jet actuator design and also to Hitachi Metals (Mr. Masuzawa) for their assistance in providing ring-shaped permanent magnets, and also Mr. Suga of Nippon Cross Atueu and Mr. Kise of Kantoc in providing the superelastic NiTi plates.

REFERENCE

1. L. Pack and R. Joslin, “Overview of Active flow control at NASA Langley Research Center”, *Proceedings of SPIE*, **3326**, pp. 202-213, 1999.
2. A. Honohan, M. Amitay and A. Glezer, “Aerodynamic Control Using Synthetic Jet”, *AIAA Fluids*, June 2000, AIAA 2000-2401, 2000.
3. M. Amitay, A. Honohan, M. Trautman, and A. Glezer, “Modification of the Aerodynamic Characteristics of Bluff Bodies Using Fluidic Actuators,” *AIAA* Paper 97-2004, June 1997.

4. B. Smith and A. Glezer, "The formation and evolution of synthetic jets", *Physics of Fluids*, **10**, No. 9, pp. 2281-2297, Sept. 1998.
5. M. Amitay, B.L. Smith, and A. Glezer, "Aerodynamic Flow Control Using Synthetic Jet Technology," *AIAA* Paper 98-0208, Jan. 1998.
6. R. Bryant, R. Fox, J. Lachowicz, and F. Chen, "Piezoelectric synthetic jets for aircraft control surfaces", *Proceedings of SPIE*, **3674**, pp. 220-227, 1999.
7. F.T. Calkins and D.J. Clingman, The Boeing Company, "Vibrating Surface Actuators for Active Flow Control", *Proceedings of SPIE,* **4698**, pp. 85-96, 2002.
8. F. T. Calkins, J.H. Mabe, J.P. Smith, and D.J. Arbogast, The Boeing Company Phantom Works, "Low frequency (F+=1.0) multilayer piezopolymer synthetic jets for active flow comtrol", *AIAA paper*, 2002-2823.
9. M. Sugiyama, R. Oshima and F.E. Fujita, *Trans. Jpn. Inst. Met*., **27**, pp. 719, 1986
10. R.D. James and W. Wuttig, "Magnetostriction of martensite", *Phil. Mag. A*, **77**, pp.1273-1299, 1998.
11. H. Kato, T. Wada, Y. Liang, T. Tagawa, M. Taya and T. Mori, "Martensite structure in polycrystalline Fe–Pd", *Materials Science and Engineering A*, **332**, pp. 134–139, 2002.
12. T. Wada, Y. Liang, H. Kato, T. Tagawa, M. Taya and T. Mori, "Structure Change and Straining in Fe-Pd polycrystals by Magnetic Field", *Mater Sci Eng-A* , v.361, pp. 75-82, 2003.
13. Y. Liang, Y. Sutou, T. Wada, C. Lee, M. Taya and T. Mori, "Magnetic Field-induced Reversible Actuation Using Ferromagnetic Shape Memory Alloys", *Scripta Mat., v*.48/10, pp. 1415-1419, 2003.
14. H. Kato, T. Wada, T. Tagawa, Y. Liang and M. Taya, "Development of Ferromagnetic Shape Memory Alloys Based on FePd alloy and Its Applications", *Proceedings of Mater. Sci. for 21th Centry, The Soc. of Mater. Sci. Japan,***Col. A**, pp.296-305, 2001.
15. Y. Liang, T. Wada, T. Tagawa and M. Taya, "Model Calculation of Stress-Strain Relationship of Polycrystalline Fe-Pd and 3D Phase transformation Diagram of Ferromagnetic Shape memory Alloys", *Proceedings of SPIE*, **4699**, pp. 206-216, 2002.
16. T. Wada and M. Taya, "Spring-based actuators", *Proceedings of SPIE*, **4699**, pp. 294-302, 2002,
17. K. Oguri, Y. Ochiai, Y. Nishi, S. Ohino and Y. Uchida, *Extended Abstracts of 9th Intelligent Materials Forum, Mitoh Science and Tech*, Tokyo, March 16, pp.24-25, 2000.
18. Y. Liang, M. Taya, Y. Kuga, "Design of diaphragm actuator based on ferromagnetic shape memory alloy composite", *Proc. of SPIE, Smart Structure and Materials, San Diego, CA, March 2-6,* V.5054, pp.45-52, 2003